BIOCHEMISTRY
including biophysical chemistry & molecular biology

Article

pubs.acs.org/biochemistry

A New Paradigm for Electron Transfer through *Escherichia coli* Nitrate Reductase A

Justin G. Fedor, Richard A. Rothery, and Joel H. Weiner*

Membrane Protein Disease Research Group, Department of Biochemistry, University of Alberta, Edmonton, Alberta T6G 2H7, Canada

Supporting Information

ABSTRACT: We have investigated the role of redox cooperativity in defining the functional relationship among the three membrane-associated prosthetic groups of *Escherichia coli* nitrate reductase A: the two hemes (b_D and b_P) of the membrane anchor subunit (NarI) and the [3Fe-4S] cluster (FS4) of the electron-transfer subunit (NarH). Previously published analyses of potentiometric titrations have exhibited the following anomalous behaviors: (i) fits of titration data for heme b_p and the [3Fe-4S] cluster exhibited two apparent components; (ii) heme b_D titrated with an apparent electron stoichiometry (n) of <1.0; and (iii) the binding of quinol oxidation inhibitors shifted the reduction potentials of both hemes despite there being only a single quinol oxidation site (Q-site) in close juxtaposition with heme b_D. Furthermore, both hemes appeared to be affected despite the absence of major structural shifts upon inhibitor binding, as judged by X-ray crystallography, or evidence of a second Q-site in the vicinity of heme b_P. In a re-examination of the redox behavior of hemes b_D and b_P and FS4, we have developed a cooperative redox model of cofactor interaction. We show that anticooperative interactions provide an explanation for the anomalous behavior. We propose that the role of such anticooperative redox behavior *in vivo* is to facilitate transmembrane electron transfer across an energy-conserving membrane against an electrochemical potential.

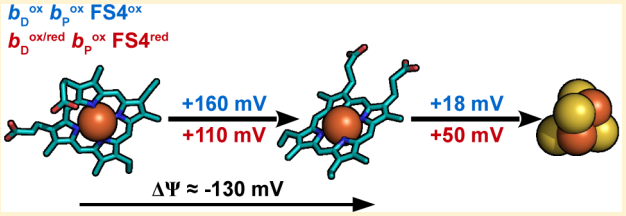

Escherichia coli nitrate reductase A (NarGHI) is a membrane-bound quinol:nitrate oxidoreductase that is expressed under anaerobic conditions in the presence of nitrate.[1] The enzyme functions as a terminal reductase where quinol oxidation is coupled to nitrate reduction, resulting in a net deposition of protons into the periplasm, which contributes to the transmembrane electrochemical gradient.[2] NarGHI comprises a nitrate-reducing subunit (NarG, 140 kDa), an electron-transfer subunit (NarH, 58 kDa), and a quinol oxidase subunit (NarI, 26 kDa). Overall, the subunits form an electron-transfer relay connecting the quinol oxidation activity of NarI to the nitrate reductase activity of NarG. NarI anchors NarGH to the cytoplasmic side of the inner membrane and binds two *b*-type hemes, one proximal (b_P) to NarGH and the other distal (b_D) from it. Electron transfer commences at the Q-site and proceeds through the two hemes (b_D then b_P) of NarI, a [3Fe-4S] cluster (FS4), three [4Fe-4S] clusters (FS1−FS3) located in NarH, and a final [4Fe-4S] cluster (FS0) and a molybdo-bis(pyranopterin guanine dinucleotide) (Mo-bisPGD) cofactor located in NarG that forms the site of nitrate reduction.[3,4] Each cofactor in the electron-transfer relay has been demonstrated to be critical for electron transfer and catalysis.[4−7] As a model system for studying biological electron transfer, NarGHI presents the advantages of robustness and being readily overexpressed in *E. coli*.[8−13]

The redox properties and reduction potentials of the NarGHI cofactors have been extensively studied using a combination of spectroscopy[10] and redox potentiometry.[11,13] EPR spectra of the hemes, FS0, FS4, and the Mo-bisPGD are well-resolved from each other, whereas those of the remaining [Fe-S] centers in NarH are complicated by spin−spin interactions.[5,6] EPR spectra of hemes b_D and b_P exhibit g_z values of approximately 3.35 and 3.75, respectively (see Figure 1). Analysis via potentiometric titrations indicates that heme b_D has an $E_{m,7}$ (reduction potential at pH 7) of 14 ± 12 mV and heme b_P has an apparent $E_{m,7}$ of approximately 118 ± 8 mV (see Table 1 of the Supporting Information and the references therein). However, the redox properties of hemes b_P and b_D and the adjacent [3Fe-4S] cluster (FS4), herein termed the transmembrane electron-transfer relay, display several abnormalities, which can be seen in Table 1 (NC rows). First, the fits to the titration data of FS4 exhibit two components, the origin of which remains unknown.[7] Second, fits to the redox titration of heme b_D are optimal with reduction occurring with a physically impossible substoichiometric number of electrons (n often approaching 0.6).[13] Finally, the binding of Q-site inhibitors, such as the menasemiquinone analogue 2-*n*-heptyl-4-hydroxyquinoline-*N*-oxide (HOQNO), pentachlorophenol (PCP), and stigmatellin, perturbs the local environment of heme b_D as manifested by altered g_z values (3.35, 3.50, 3.45, and 3.31 for unbound, HOQNO-bound, PCP-bound, and stigmatellin-bound enzymes, respectively).[13−15] The g_z value of heme b_P, however, is unaltered in each case, and a crystal structure of

Received: March 31, 2014
Revised: June 10, 2014
Published: June 24, 2014

   dx.doi.org/10.1021/bi500394m | *Biochemistry* 2014, 53, 4549−4556

the PCP-bound form and a model of the HOQNO-bound enzyme reveal no significant structural perturbations around heme b_P.[15] Furthermore, enzyme kinetics, EPR, and binding assays are consistent with the presence of a single Q-site in close juxtaposition with heme b_D.[7,13−24] Interestingly though, HOQNO binding influences the apparent reduction potentials of both hemes, with that of heme b_D increasing from ∼20 to ∼120 mV and that of heme b_P decreasing from ∼120 to ∼60 mV.[7] The anomalies described above indicate that our understanding of transmembrane electron flow through NarGHI is substantially incomplete.

In this paper, we demonstrate a model describing electronic interactions among the three prosthetic groups of the transmembrane electron-transfer relay of NarGHI that explains their apparently anomalous behaviors. This model also describes a mechanism for enhanced electron transfer against a transmembrane electrochemical potential and possibly a mechanism for gated electron flow into NarGHI.

METHODS

Bacterial Strains, Plasmids, and Membrane Vesicle Preparation. Wild-type NarGHI was overexpressed in *E. coli* strain LCB79 [*araD*139 Δ(*lac*I-POZYA-*argF*) *rpsL*, *thi*, Φ79(*nar-lac*)].[25] pVA700 (*tacP*, *rrnB*, *lacI*^{q}, amp^r, *narGHJI*) was used as the expression vector.[6] Vector pCD7 (*tacP*, *rrnB*, *lacI*^{q}, amp^r, *narI*) was used to express NarI(ΔGH).[16] Growth in flasks and vesicle preparation methods were conducted as previously described, and the inner membrane fraction was obtained via differential ultracentrifugation (40000 rpm, 1.5 h) using a 55% (w/v) sucrose step gradient as previously described.[13] The buffer system used for vesicle preparation consisted of 100 mM MOPS and 5 mM EDTA (pH 7.0).

Redox Potentiometry and EPR Spectroscopy. Redox titrations were conducted under argon at 25 °C in 100 mM MOPS and 5 mM EDTA (pH 7.0) as previously described.[13,26] The titrations were conducted in the reducing direction, and often several points were taken in the oxidizing direction, as well. We did not find any appreciable hysteresis in the titrations. Titrations in the presence of HOQNO, PCP, and stigmatellin were conducted using inhibitor concentrations of 0.5, 1, and 0.3 mM, respectively. All samples were prepared in 3 mm inner diameter quartz EPR tubes, rapidly frozen using liquid nitrogen-chilled ethanol, and stored under liquid nitrogen prior to use. EPR spectra were acquired as previously described[13] using a Bruker ESP300 spectrometer (9.47 GHz) with ESR-900 flowing helium cryostat, a temperature of 12 K, and a 19 G_{pp} modulation amplitude at 100 kHz at 20 mW microwave power for the stigmatellin and 100 mW microwave power for the HOQNO titrations. The wild-type and PCP-bound spectra were recorded using a Bruker Elexsys E500 series X-band EPR spectrometer (9.38 GHz) with an ESR-900 flowing helium cryostat, a temperature of 12 K, a 10 G_{pp} modulation amplitude at 100 kHz, and a 20 mW microwave power. All potentials mentioned are relative to the standard hydrogen electrode. All FS4 data were acquired at 10 dB, with signal intensity taken from g = 1.997 minus the trough intensity at g = 1.973.

Fitting and Modeling of Redox Titration Data. To model the redox interactions in the system comprising hemes b_D and b_P and FS4, we used a model diagrammatically depicted in Figure 2A and mathematically outlined in Figure 1 of the Supporting Information.[27,28] To apply the model to the data, we assigned center A as heme b_D, center B as heme b_P, and center C as FS4. To model the system comprising just the two hemes, a simplified model was used in which just E_mA, E_mB, and *e*AB were used (Figure 2B).

In applying this model to the data, we assume there are no interactions between the hemes or FS4 and the other centers in NarGHI, including bound quinone species, and only interactions between adjacent centers are considered. Matlab (version R2013b, The MathWorks Inc., Natick, MA) was used to conduct nonlinear least-squares fitting of the model to the data by reducing the sum of squares between theoretical fits and experimental data points, where the reduction and interaction potentials, baseline and scale, were allowed to vary. The maximum and baseline of the titration curves were limited to ±5% variation. The qualities of the fits were calculated in MatLab to yield the correlation coefficients, as well as 95% confidence intervals and standard errors in the modeled parameters. In each case, fits achieved a correlation coefficient of ≥98%. The raw data for the K86A, stigmatellin, HOQNO, and NarI(ΔGH) titrations used in this study were previously published but reprocessed and reanalyzed.[13]

RESULTS AND DISCUSSION

Sample and Data Considerations. EPR is an excellent technique for the study of electron-transfer relays containing cofactors with well-resolved spectral features. The oxidized hemes of the NarGHI transmembrane electron-transfer relay are readily resolved, with heme b_P having a g_z of approximately 3.75 and heme b_D having a g_z of approximately 3.35. The spectrum of oxidized FS4 is also well resolved from those of the other centers of the enzyme and comprises a peak (g_z) at g = 2.02 and a peak to trough (g_{xy}) immediately upfield at g = 1.99. However, before their behavior in the potential domain can be thoroughly analyzed, the homogeneity of these signals needs to be established. The g = 3.75 peak of heme b_D is clearly resolved from signals of other moieties that might impact our analyses (Figure 1), as there are no signals in this region in membranes lacking NarGHI.[16,18,29,30] FS4 is more complicated, because FS1 can interfere with the signal interpretation as can the presence of extraneous background iron−sulfur clusters. It has previously been shown, however, that the NarH−FS4 species is by far the predominant species and that only at low potentials does FS1 begin to interfere.[6,7,12,13] The nearest signal due to FS1 appears at g = 2.013, and the background signal exhibits a peak at 2.02, which overlaps with the dominant signal of FS4 at 2.021. These examples of signal interference can be mitigated by measuring the FS4 signal intensity at g = 1.997 minus the trough intensity at 1.973, as depicted by the inverted black triangles in Figure 1.

Interpretation of the heme b_D EPR signal poses the most significant challenge. Heme b_D often manifests as having two subpopulations with g_z values of ∼3.35 and ∼3.2, which we propose are due to differential Q-site occupancies,[30] whereas others have suggested the subpopulations arise from differential cardiolipin occupancies.[31] Under anaerobic or microaerobic conditions, the g_z feature of the heme b_D spectrum manifests as a single peak at g = 3.35 (Figure 1).[13,16,30] When present, these two subpopulations do exhibit different apparent reduction potentials, and thus, simple signal integration is not feasible.[30] However, the two subpopulations collapse into one signal, albeit with a shifted g_z, upon inhibitor binding. In the case of HOQNO, PCP, and stigmatellin binding, the g_z value for heme b_D shifts from 3.35 to 3.50, 3.45, and 3.31, respectively.[13−15] Likewise, the NarGHI^{K86A} Q-site variant not only exhibits a

dx.doi.org/10.1021/bi500394m | *Biochemistry* 2014, 53, 4549−4556

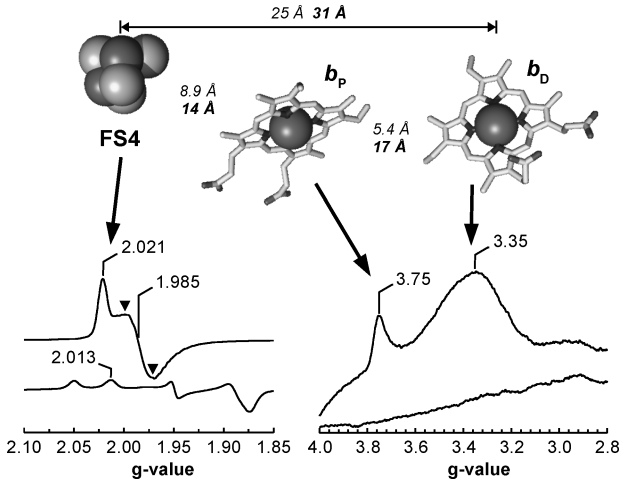

Figure 1. Transmembrane electron-transfer relay of NarGHI comprising hemes b_D and b_P and FS4 and their representative EPR spectral features. The distances between cofactors are given as edge-to-edge (italics) and center-to-center (bold) values. Representative pH 7.0 EPR spectra (9.47 GHz) at 12 K of FS4 (10 dB) and hemes b_D (g_z = 3.35) and b_P (g_z = 3.75) (17 dB) fully oxidized (286 mV) and fully reduced (−67 mV for hemes and −8 mV for FeS). The inverted triangles denote the intensity measurement for the FS4 signal at g values of 1.997 and 1.973. This image was generated using PyMol[43] and Protein Data Bank entry 1Q16.[4]

homogeneous heme b_D EPR signal at ∼3.3 but also exhibits reduced quinol oxidase activity and is unable to bind HOQNO or stabilize a semiquinone radical.[15,18,30] Using the inhibitor-bound states also addresses the possibility, and likely inevitability, of interactions of the adjacent heme (b_D) with the bound quinone species, particularly the stable anionic semiquinone.[19,32] For the reasons described above, we focus our analyses herein on the more homogeneous inhibitor-bound states and the NarGHI^{K86A} Q-site variant.

Redox Titrations of FS4 and Hemes b_D and b_P. The basic Nernst equation is normally applied in analyzing redox titration data (Figure 3A, dashed lines).[28] However, close examination of previous titrations reveals a couple of redox titration anomalies for components of the NarGHI transmembrane electron-transfer relay. (i) To adequately fit the titration data for FS4, two components of E_m (186 and 83 mV) are required (Table 1), essentially in agreement with published values.[7,12,13] Compare the fits in Figure 3 for FS4, where the broadly dashed lines represent idealized Nernstian fits (n = 1 and one component) and the finely dashed lines are fits where two n = 1 components are utilized. The residuals (Figure 3 of the Supporting Information) clearly show that FS4 is better fit by the two components rather than a single component. (ii) While previously published titration data for heme b_P utilized n = 1 fits,[13] the curves can be better modeled with an apparent electron stoichiometry significantly below unity. Again, this can be seen in Figure 3 (and Table 1) where the broadly dashed lines represent idealized Nernstian fits (n = 1) and the more finely dashed lines are modified models in which the apparent n

Table 1. Cooperative (C) and Noncooperative (NC) Fitting Parameters[a] for Redox Titrations of Nitrate Reductase Preparations As Seen in Figure 3

		E_m[a,c] Heme b_D (mV)	E_m[a,c] Heme b_P (mV)	E_m[a,b] [3Fe-4S] (mV)	e[d] b_D-b_P (mV)	e[d] b_P-[3Fe-4S] (mV)
Wild Type	NC1	+2 ± 5	+128 ± 5	+163 ± 5	0	0
	NC2	+2 ± 5	+129 ± 5 (n = 0.64)	+186 ± 5 (75%) +83 ± 18 (25%)	0	0
	C	+3 ± 4	+163 ± 5	+181 ± 4	0	-50 ± 7
K86A	NC1	+12 ± 8	+88 ± 2	+182 ± 4	0	0
	NC2	+12 ± 8	+88 ± 2	+195 ± 3 (84%) +85 ± 16 (16%)	0	0
	C	+15 ± 3	+131 ± 8	+186 ± 3	0	-45 ± 9
+ 0.5 mM HOQNO	NC1	+109 ± 6	+51 ± 5	+174 ± 5	0	0
	NC2	+106 ± 5 (n = 0.6)	+52 ± 8 (n = 0.8)	+196 ± 6 (74%) +105 ± 19 (26%)	0	0
	C	+120 ± 4	+142 ± 9	+182 ± 4	-49 ± 7	-46 ± 10
+ 0.3 mM Stigmatellin	NC1	+35 ± 2	+115 ± 6	+167 ± 7	0	0
	NC2	+35 ± 2	+115 ± 5 (n = 0.56)	+197± 4 (70%) +94 ± 10 (30%)	0	0
	C	+58 ± 6	+166 ± 4	+187 ± 3	-27 ± 8	-62 ± 5
+ 1 mM PCP	NC1	-38 ± 3	+73 ± 2	+178 ± 3	0	0
	NC2	-38 ± 3	+73 ± 2	+190 ± 2 (89%) +88 ± 16 (11%)	0	0
	C	-38 ± 2	+120 ± 7	+184 ± 2	0	-49 ± 7
pCD7	NC	+40 ± 3	-180 ± 5	N.A.	0	N.A.
	C	+39 ± 3	-180 ± 4	N.A.	0	N.A.

[a]MatLab-modeled fits are represented as means ± the standard error. [b]E_m values correspond to reduction potentials at pH 7. [c]The noncooperative values represent macroscopic E_m values, where the percentage denotes the contribution of the single component in multicomponent fits. [d]Unless specified, fits were generated using electron stoichiometries of n = 1. [e]e is the cooperative component of the system and quantifies the interactions between the two specified adjacent cofactors. [f]Not applicable.

dx.doi.org/10.1021/bi500394m | *Biochemistry* 2014, 53, 4549−4556

is <1 (see the residuals in Figure 3 of the Supporting Information). Critically, this behavior is dependent upon the variant studied, the presence of Q-site inhibitors, and the subunit composition of the preparation studied. For example, data obtained from the NarGHI^{K86A} variant, the wild-type enzyme in the presence of PCP, and the NarI subunit expressed by itself [NarI(ΔGH)] can be fit to n = 1 Nernstian curves (see Table 1 and Figure 3B, D, F).[13,18] In contrast to the behavior of heme b_P, reduction of heme b_D is described well by n = 1 fits. The heme b_D titrations depicted in panels A, B, and D of Figure 3 do have a minor extraneous component modeled at 157 ± 2 mV, which has been attributed to the overlapping spectrum of heme b_{558} of cytochrome *bd*.[16,27,30,33]

A further peculiarity of the NarGHI transmembrane electron-transfer relay is that the Q-site inhibitor HOQNO elicits an apparent inversion of the reduction potentials of the two hemes and has a modest effect on the lower-potential component of FS4 [shifting it from approximately 83 to 105 mV (Figure 3C and Table 1)]. Interestingly, this is accompanied by the titration of heme b_P taking on a more ideal n = 1 behavior while heme b_D exhibits an apparent n = 0.6 fit (Table 1).

Together, these observations could be explained by NarI containing multiple quinone binding sites or the fact that HOQNO binding induces structural changes in the enzyme and consequently shifts the E_m values for both hemes. However, we and others have shown by HOQNO fluorescence quench titrations, EPR spectroscopy, and X-ray crystallography that there is only a single quinol binding site in the enzyme, found adjacent to heme b_D, which binds both menaquinone and ubiquinone as well as Q-site inhibitors PCP, HOQNO, and stigmatellin.[13,15,18−20] Furthermore, a crystal structure with PCP bound to NarI has been determined,[15] and modeling HOQNO into the position taken by PCP reveals that there are no significant actual or predicted conformational changes in the vicinity of heme b_P elicited by inhibitor binding. It is thus unlikely that the redox behavior of heme b_P and FS4 in the HOQNO-bound state is due to a second Q-site or inhibitor binding-induced changes in conformation. There is also no published evidence of appreciable redox-dependent conformational changes in NarGHI. Thus, the nonideal redox behavior of NarGHI is unlikely to be due to redox-dependent conformational changes. We therefore posit that the underlying cause is the existence of anticooperative redox interactions between the cofactors.

Modeling Redox Cooperativity. It is known that surface charges as well as charged residues and dipole moments within proteins influence the reduction potentials of embedded cofactors, which are analogous to the factors that influence the pK_a values of amino acid residues.[34,35] Because reduction of a cofactor can readily change its overall charge, it can also elicit electrostatic effects on adjacent cofactors, thereby modulating their reduction potentials.[36,37] This is manifested in the observation of positive (n > 1) or negative (n < 1) cooperativity. For a system exhibiting positive cooperativity, reduction of a cofactor increases the reducibility (increases E_m) of adjacent cofactors. Conversely, negative cooperativity (anticooperativity) is such that reduction of one cofactor decreases the reducibility (reduces E_m) of the others. Thus, cooperativity is a plausible explanation for the observation of non-Nernstian redox chemistry within the transmembrane electron-transfer relay of NarGHI. A notable example of an anticooperative redox interaction is that between hemes b_{558} and b_{595} of *E. coli* cytochrome *bd*, wherein apparent n values of 0.7−0.9 were required for satisfactory fits using standard Nernstian models. Similar quality fits were obtained by modeling an anticooperative interaction of −32 mV between these two cofactors.[27]

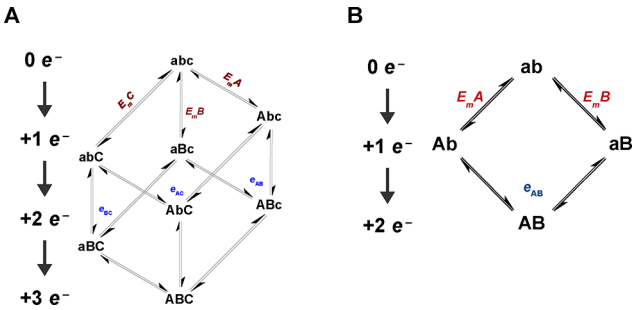

Figure 2. Thermodynamic model for NarGHI hemes b_D and b_P and FS4 depicted schematically. E_m is the given reduction potential of the given cofactor A, B, or C, and the interaction potentials are depicted as variables e_{AB}, e_{BC}, and e_{AC} for interactions between the specified cofactors. Lowercase letters (a−c) indicate an oxidized state, whereas uppercase letters denote reduction by a single electron, where A = b_D, B = b_P, and C = FS4. See the text for a full description of the model; the specific equations used can be found in Figure 1 of the Supporting Information.

To explain the anomalous behavior of the NarGHI transmembrane electron-transfer relay, we applied a three-center model with pairwise interactions between adjacent centers. The thermodynamic model for the transmembrane electron-transfer relay, consisting of hemes b_D and b_P and FS4, is depicted schematically in Figure 2A (see Figure 1 of the Supporting Information for mathematical details). In the scheme, E_m is the reduction potential of the given center (A) b_D, (B) b_P, or (C) FS4, and the interaction potentials are depicted as variables e_{AB}, e_{BC}, and e_{AC}, denoting an interaction between the specified centers. Lowercase letters (a−c) indicate an oxidized state, whereas uppercase letters (A−C) denote reduction by a single electron. To prevent overparametrization of the fittings, we looked only at pairwise interactions; therefore, e_{AC} was fixed at 0 mV. This is reasonable if the cooperativity is purely electrostatic, because the inverse distance dependence of the electrostatic interaction energy would ensure the long-range interaction between centers FS4 and b_D (edge-to-edge distance of ∼25 Å) would be negligible in comparison to the much more proximal pairwise interactions (b_P−FS4 distance of 8.9 Å; b_D−b_P distance of 5.4 Å) (see Figure 1).[4] As a reminder, the heme b_D titrations depicted in panels A, B, and D of Figure 3 do have a minor extraneous component modeled at 157 ± 2 mV, which is due to heme b_{558} of cytochrome *bd*, and consequently, this high-potential component of the titrations of b_D was not included in the cooperativity model.[16,27,30,33]

Applying the Model to the Redox Titrations of Hemes b_D and b_P and FS4. Table 1 summarizes the fitting parameters used for the noncooperative and cooperative models for the inhibitor-free, HOQNO-bound, PCP-bound, and stigmatellin-bound states of NarGHI, and the corresponding redox titrations are depicted in Figure 3. Broadly dashed lines represent single-component standard Nernstian fits where n = 1. The finely dashed lines represent multicomponent Nernstian fits or fits where the apparent n value is <1. The solid lines

dx.doi.org/10.1021/bi500394m | *Biochemistry* 2014, 53, 4549−4556

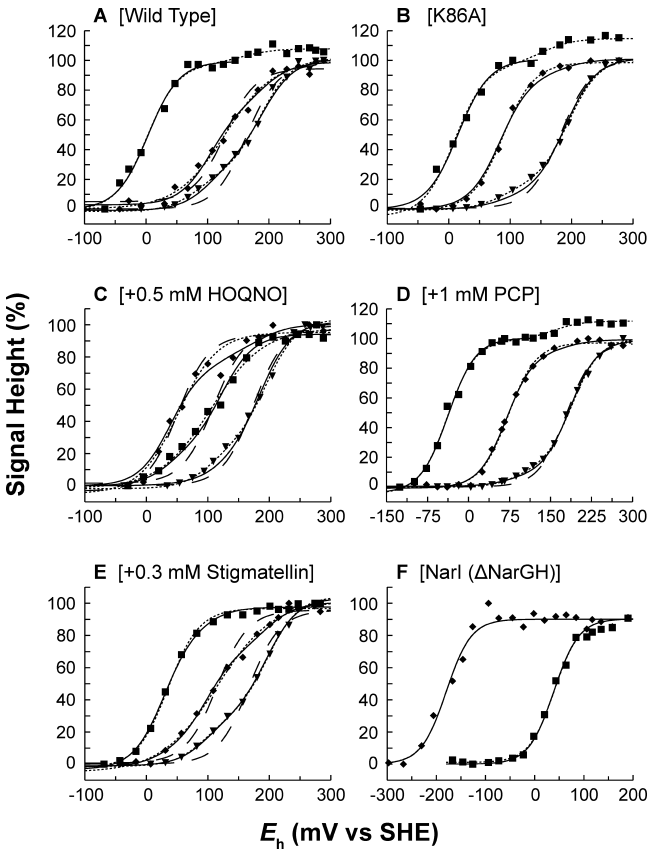

Figure 3. Fits for the redox titrations of hemes b_D (■) and b_P (◆) and FS4 (▼). Broadly dashed lines (– – –) denote "standard" Nernstian fits in which a single n = 1 component is modeled. Finely dashed lines (---) denote modified Nernstian fits in which either two components or apparent n values of <1 are used as the model. Solid lines (—) denote fits by the cooperative models depicted in Figure 2. See Table 1 for the respective fitting parameters used. The applied potential (E_h) is relative to the standard hydrogen electrode, and the signal intensities are normalized to 100%. Titrations A, B, and D include fits of 160, 156, and 155 mV, respectively, to account for the contaminating b_{558} of cytochrome *bd* in the membrane preparations. The redox titrations correspond to vesicle preparations of (A) wild-type NarGHI, (B) NarGHI^{K86A}, (C) NarGHI supplemented with 0.5 mM HOQNO, (D) NarGHI in the presence of 1 mM PCP, (E) NarGHI supplemented with 0.3 mM stigmatellin, and (F) NarI(ΔNarGH) membranes.

represent fits derived from the cooperative model depicted in Figure 2A (see the Supporting Information for additional details). The residuals are plotted in Figure 3 of the Supporting Information.

We favor the cooperative model over those invoking multiple components and apparent n values of <1 because similar quality fits are obtained using fewer parameters. For example, the multiple-component fit for the wild-type inhibitor-free bound enzyme has seven degrees of freedom, whereas the cooperative fit has only five. However, it does appear that certain sections of the titrations, particularly the low-potential end of FS4 titrations, are better fit with the modified Nernstian models than the cooperative model. Our model utilizes only pairwise interactions and does not take into account interactions with other cofactors within the protein, including the bound quinone. We have found that modeling the interaction between heme b_D and FS4 gave slightly better fits (data not shown); however, the increased number of parameters resulted in a greatly diminished level of confidence in the fits, and as a consequence, we decided to look at only adjacent pairwise interactions. Therefore, the model has the ability to account for multiple components for FS4 and shallower titration slopes for b_D (and b_P in the HOQNO-bound state) but is not sophisticated enough to account for all the more subtle effects we observe in the redox titrations of the transmembrane electron-transfer relay.

The most evident pairwise interaction is between heme b_P and FS4, with an average between all samples of −50 ± 7 mV. This interaction manifests as substoichiometric apparent n values for heme b_P and multiple apparent redox components for FS4 titrations, and it has previously been suggested that a mutual redox interaction is responsible for this behavior.[7] However, there is a weaker apparent interaction between the two hemes despite the distances between b_D and b_P being similar to the separation of FS4 and b_P (see Figure 1). One reasonable explanation for this would be that the charge density is higher in iron−sulfur clusters than in hemes, because the electron density of reduced hemes is known to extend over the entire porphyrin macrocycle.[38,39] To eliminate the supposed effects of the FS4−b_P interaction on heme the b_P line shape, we re-examined the published EPR spectra of NarI expressed in the absence of NarGH where heme b_P undergoes a shift in its g value from 3.75 to 2.92 and a decrease in $E_{m,7}$ of >100 mV.[13] With the large divergence in reduction potentials between the two hemes, no obvious redox interaction was discerned and the b_P−b_D interaction was therefore set to zero. In agreement with the hypothesis that the nonideal redox titration curve of heme b_P is due to redox interactions with heme b_D and FS4, we observe only ideal n = 1 single-component Nernstian redox titrations of the two hemes (Figure 3F).

In the case of b_D−b_P interaction, there is a dependence of interaction energy on the apparent difference in reduction potentials. In most cases, the E_m values for hemes b_D and b_P are divergent enough that the titration curve effects indicative of redox cooperativity, such as slope shallowing or multiple apparent components, are not present, and therefore, an interaction potential was not measurable. The two instances in which this was not the case are the titrations of the HOQNO- and stigmatellin-bound states. In the stigmatellin titration, a b_D−b_P interaction potential of −27 mV was determined and the corresponding divergence in E_m values of the two hemes was ∼100 mV. Contrast this with the wild-type inhibitor-free heme E_m difference of 160 mV. In the HOQNO titration, the heme E_m difference is a mere 20 mV and the magnitude of the interheme interaction (−49 mV) approaches that of the heme b_P−FS4 interaction (−50 mV).

Fitting redox titrations of the transmembrane electron-transfer relay to the model presented also gives us an alternative perspective on the effects of HOQNO binding. Previously, HOQNO was thought to modify the E_m values of hemes b_D and b_P such that heme b_D exhibits an E_m higher than that of b_P. This is concurrent with HOQNO eliciting a significant shallowing of the titration curve of b_D.[13] Utilizing the cooperative model, heme b_P does experience an increase in its E_m; however, it remains lower than that of heme b_D. This is expected because HOQNO binds adjacent to, and therefore changes the g_z value of, heme b_D and not heme b_P, and models based on the PCP-bound structure indicate a lack of HOQNO-induced conformational changes in NarI.[13−15] In the context of cooperativity, the E_m of heme b_P is only diminished by 20 mV; however, the heme b_D reduction potential and b_D−b_P interaction are modulated upon HOQNO binding. The

dx.doi.org/10.1021/bi500394m | *Biochemistry* 2014, 53, 4549−4556

interaction potential between the two hemes varies significantly between the inhibited states of the enzyme, but as the E_m of heme b_P and FS4 remains largely unchanged, so too does the interaction energy between these two centers. Similar phenomena are observed in the PCP and stigmatellin titrations where principally the E_m of heme b_D is influenced. Again, this is consistent with a single Q-site and the conformational integrity of NarI regardless of whether inhibitors are bound or absent. Modulation of the b_D–b_P interaction may be due to the effects of inhibitor binding on the electrostatic environment around and between these two hemes and/or simply the fact that as the E_m values of the hemes become more divergent, it becomes more difficult to determine the magnitude of their interaction.

Functional Consequences of Redox Anticooperativity in NarGHI. The phenomenon of redox anticooperativity in NarGHI would explain the two-phase reoxidation kinetics previously observed for NarGHI, particularly in the presence of HOQNO, where the slower reoxidation phase becomes significantly more pronounced (see ref 7 for details). That is, HOQNO predominantly modulates the heme b_D E_m and b_D–b_P interaction, such that the macroscopic E_m of b_P appears to be lower than that of b_D. It is the anticooperative b_D–b_P interaction and the increased b_D reduction potential that slow electron transfer through NarI.

Redox interactions within NarGHI may actually have implications in the broader context of bacterial respiration. Because of the orientation of NarGHI in the membrane, electron flow through NarI is from the P-side of the membrane (heme b_D) to the N-side (heme b_P) and therefore is against the transmembrane potential, $\Delta\Psi$, which is approximately −130 mV in nitrate-respiring *E. coli*.[40] Considering the previously reported values of 14 and 118 mV for hemes b_D and b_P, respectively, the ΔE of 104 mV is insufficient to overcome the transmembrane potential (see Figure 4A). However, Figure 4B demonstrates that when considering the values modeled herein of 3 mV for b_D and 163 mV for b_P, the resultant ΔE of 160 mV is sufficiently compensatory for the transmembrane potential. Similarly, the presence of a membrane potential has been shown to have large effects on electron transfer and the distribution between hemes b_{556} and b_{562} of cytochrome bc_1.[41,42]

It is also possible that the major functional consequence of electrostatic interactions in the transmembrane electron-transfer relay may be to gate electron flow through NarI. Figure 4B shows the energetics of transmembrane electron transfer when the system is fully oxidized (top) or when FS4 (and b_D) is reduced (bottom). The reduction of FS4 brings the inter-heme electron-transfer potential, that is from b_D to b_P, from 160 to 110 mV, due to the lowering of the E_m of b_P by b_P–FS4 anticooperativity (−50 mV). When $\Delta\Psi$ is taken into account, the ΔE for transmembrane electron transfer decreases from 30 mV when FS4 is oxidized to −20 mV when FS4 is reduced. Consequently, during steady-state turnover of the enzyme and upon reduction of FS4, b_D has a stronger propensity to remain reduced. It has been previously shown that reduction of NarI decreases the K_m for HOQNO from 0.34 to 0.07 μM, thus ensuring tighter binding of HOQNO, and supposedly the semiquinone intermediate.[7] Such an effect has been observed for cytochrome bc_1, where Q_o semiquinone stability is directly coupled to b_{562} reduction (the adjacent heme) and semiquinone stability increases further when b_{566} is reduced.[41] By more tightly binding and stabilizing the semiquinone, the enzyme may physically prevent entry of

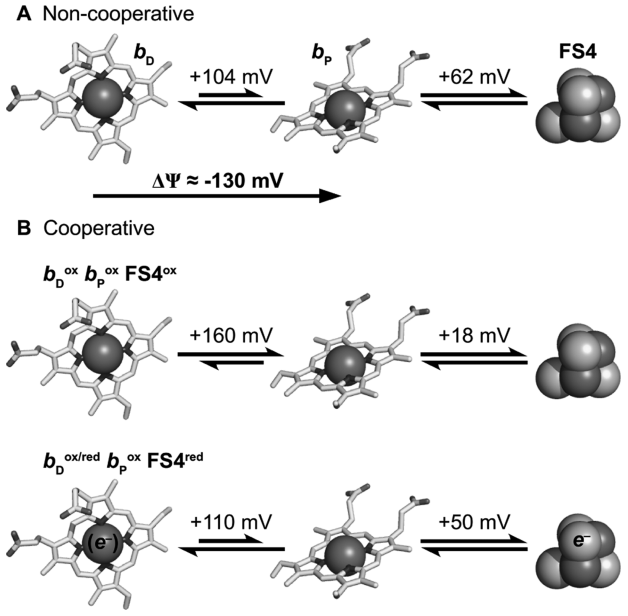

Figure 4. Electron-transfer across the plasma membrane from b_D to FS4 using the old and new paradigm for the transmembrane electron-transfer relay of NarGHI. The equilibrium arrows between b_D and b_P indicate the direction of favorable electron transfer when $\Delta\Psi$, −130 mV, is considered.[40] Panel A depicts the current paradigm of electron transfer through the transmembrane electron-transfer relay using the average published $E_{m,7}$ values for b_D, b_P, and FS4 of 14, 118, and 180 mV, respectively, as mentioned in the text. Panel B depicts the thermodynamics of electron transfer through the transmembrane electron-transfer relay where the revised potentials and interactions are considered where the potentials used for b_D, b_P, FS4, eb_D–b_P, and eb_P–FS4 are 3, 163, 181, 0, and −50 mV, respectively. Three states are considered: the first in which the system is fully oxidized and the second and third in which FS4 is reduced and FS4 and b_D are reduced, respectively. When FS4 is reduced, the apparent E_m of b_P decreases to 113 mV (a loss of 50 mV). This results in mildly unfavorable electron flow across the membrane and increased electron residence on heme b_D, the effects of which may include tighter binding of the semiquinone and thus blocked entrance of further reducing equivalents into NarGHI.

further reducing equivalents. Therefore, by decreasing the potential for transmembrane electron transfer under nitrate-limiting conditions, the anticooperativity within NarI may facilitate more effective usage of the Q-pool by diverting quinol to the other terminal reductases, such as those for DMSO, TMAO, and fumarate reductase.

A further consideration is that the model addresses only part of the entire NarGHI electron-transfer relay that comprises eight cofactors (two hemes, five [Fe-S] clusters, and a molybdenum cofactor) and the reactants. The span of reduction potentials in NarGHI is rather large (from −400 to 200 mV), but with the number of cofactors present, the midpoint potential overlap is considerable.[4] Also, redox cooperativity would have significant implications for quinol binding and oxidation as well as semiquinone stabilization. Therefore, to have a complete thermodynamic picture of NarGHI, it would be insightful to extend the current model to include all other redox cofactors, including quinone and nitrate binding and redox transitions. One example is the very low potential [4Fe-4S] cluster FS2 in NarH that has a measured $E_{m,7}$ of −420 mV; it may be that the measured E_m is so low because of electrostatic interactions with adjacent reduced

dx.doi.org/10.1021/bi500394m | *Biochemistry* 2014, 53, 4549–4556

cofactors and that the microscopic midpoint potential is actually higher.[8]

In summary, we have shown that the nonideal Nernstian redox titration curves for hemes b_D and b_P and FS4 in the Q-site inhibitor-bound state can be modeled as arising from anticooperative electrostatic interactions among these cofactors. We were able to satisfactorily fit the redox titrations with a model that includes E_m values and pairwise interactions between adjacent cofactors. Importantly, by modeling NarGHI redox cofactor thermodynamics in the frame of redox cooperativity, we obtain values significantly different from those previously reported, particularly for heme b_P, providing an alternative perspective on electron-transfer thermodynamics in the NarGHI system and shedding light on inhibitor binding effects and a functional role for these electrostatic interactions in electron transfer through NarI in the presence of an electrochemical gradient.

■ ASSOCIATED CONTENT

Supporting Information

Equations utilized in modeling the redox titrations as well as the plotted residuals of the titrations depicted in Figure 3. This material is available free of charge via the Internet at http://pubs.acs.org.

■ AUTHOR INFORMATION

Corresponding Author

*Department of Biochemistry, University of Alberta, Edmonton, Alberta T6G 2H7, Canada. E-mail: joel.weiner@ualberta.ca. Phone: (780) 492-2761 (office). Phone: (780) 492-2558 (lab). Fax: (780) 492-0886.

Funding

This work was funded by the Canadian Institutes of Health Research (MOP, 106550). J.G.F. was supported by studentships from the Killam Trusts Foundation and Alberta Innovates: Health Solutions.

Notes

The authors declare no competing financial interest.

■ ACKNOWLEDGMENTS

We thank Francesca Sebastian and Shannon Murphy for technical assistance as well as the rest of the Weiner laboratory for their helpful comments and discussions.

■ ABBREVIATIONS

b_D, *b* heme distal to NarGH; b_P, *b* heme proximal to NarGH; C, cooperative; EPR, electron paramagnetic resonance; E_h, applied potential; $E_{m,X}$, reduction potential at pH *X*; HOQNO, 2-*n*-heptyl 4-hydroxyquinoline-*N*-oxide; NarGHI, *E. coli* nitrate reductase A; NC, noncooperative; FS4, [3Fe-4S]; PCP, pentachlorophenol.

■ REFERENCES

(1) Wimpenny, J. W. T., and Cole, J. A. (1967) The regulation of metabolism in facultative bacteria III. The effect of nitrate. *Biochim. Biophys. Acta 148*, 233−242.

(2) Richardson, D. J., and Watmough, N. J. (1999) Inorganic nitrogen metabolism in bacteria. *Curr. Opin. Chem. Biol. 3*, 207−219.

(3) Blasco, F., Guigliarelli, B., Magalon, A., Asso, M., Giordano, G., and Rothery, R. A. (2001) The coordination and function of the redox centres of the membrane-bound nitrate reductases. *Cell. Mol. Life Sci. 58*, 179−193.

(4) Bertero, M. G., Rothery, R. A., Palak, M., Hou, C., Lim, D., Blasco, F., Weiner, J. H., and Strynadka, N. C. (2003) Insights into the respiratory electron transfer pathway from the structure of nitrate reductase A. *Nat. Struct. Biol. 10*, 681−687.

(5) Augier, V., Guigliarelli, B., Asso, M., Bertrand, P., Frixon, C., Giordano, G., Chippaux, M., and Blasco, F. (1993) Site-directed mutagenesis of conserved cysteine residues within the β subunit of *Escherichia coli* nitrate reductase. Physiological, biochemical, and EPR characterization of the mutated enzymes. *Biochemistry 32*, 2013−2023.

(6) Guigliarelli, B., Magalon, A., Asso, M., Bertrand, P., Frixon, C., Giordano, G., and Blasco, F. (1996) Complete coordination of the four Fe-S Centers of the β subunit from *Escherichia coli* nitrate reductase. Physiological, biochemical, and EPR characterization of site-directed mutants lacking the highest or lowest potential [4Fe-4S] clusters. *Biochemistry 35*, 4828−4836.

(7) Rothery, R. A., Blasco, F., and Weiner, J. H. (2001) Electron transfer from heme b_L to the [3Fe-4S] cluster of *Escherichia coli* nitrate reductase A (NarGHI). *Biochemistry 40*, 5260−5268.

(8) Guigliarelli, B., Asso, M., More, C., Augier, V., Blasco, F., Pommier, J., Giordano, G., and Bertrand, P. (1992) EPR and redox characterization of iron-sulfur centers in nitrate reductases A and Z from *Escherichia coli*. Evidence for a high-potential and a low-potential class and their relevance in the electron-transfer mechanism. *Eur. J. Biochem. 207*, 61−68.

(9) Johnson, M. K., Bennett, D. E., Morningstar, J. E., Adams, M. W., and Mortenson, L. E. (1985) The iron-sulfur cluster composition of *Escherichia coli* nitrate reductase. *J. Biol. Chem. 260*, 5456−5463.

(10) Hackett, N. R., and Bragg, P. D. (1982) The association of two distinct *b* cytochromes with the respiratory nitrate reductase of *Escherichia coli*. *FEMS Microbiol. Lett. 13*, 213−217.

(11) Magalon, A., Rothery, R. A., Giordano, G., Blasco, F., and Weiner, J. H. (1997) Characterization by electron paramagnetic resonance of the role of the *Escherichia coli* nitrate reductase (NarGHI) iron-sulfur clusters in electron transfer to nitrate and identification of a semiquinone radical intermediate. *J. Bacteriol. 179*, 5037−5045.

(12) Rothery, R. A., Magalon, A., Giordano, G., Guigliarelli, B., Blasco, F., and Weiner, J. H. (1998) The molybdenum cofactor of *Escherichia coli* nitrate reductase A (NarGHI). Effect of a *mobAB* mutation and interactions with [Fe-S] clusters. *J. Biol. Chem. 273*, 7462−7469.

(13) Rothery, R. A., Blasco, F., Magalon, A., Asso, M., and Weiner, J. H. (1999) The hemes of *Escherichia coli* nitrate reductase A (NarGHI): Potentiometric effects of inhibitor binding to narI. *Biochemistry 38*, 12747−12757.

(14) Magalon, A., Rothery, R. A., Lemesle-Meunier, D., Frixon, C., Weiner, J. H., and Blasco, F. (1998) Inhibitor binding within the NarI subunit (cytochrome b_{nr}) of *Escherichia coli* nitrate reductase A. *J. Biol. Chem. 273*, 10851−10856.

(15) Bertero, M. G., Rothery, R. A., Boroumand, N., Palak, M., Blasco, F., Ginet, N., Weiner, J. H., and Strynadka, N. C. (2005) Structural and biochemical characterization of a quinol binding site of *Escherichia coli* nitrate reductase A. *J. Biol. Chem. 280*, 14836−14843.

(16) Magalon, A., Lemesle-Meunier, D., Rothery, R. A., Frixon, C., Weiner, J. H., and Blasco, F. (1997) Heme axial ligation by the highly conserved His residues in helix II of cytochrome *b* (NarI) of *Escherichia coli* nitrate reductase A. *J. Biol. Chem. 272*, 25652−25658.

(17) Rothery, R. A., Chatterjee, I., Kiema, G., McDermott, M. T., and Weiner, J. H. (1998) Hydroxylated naphthoquinones as substrates for *Escherichia coli* anaerobic reductases. *Biochem. J. 332* (Part1), 35−41.

(18) Lanciano, P., Magalon, A., Bertrand, P., Guigliarelli, B., and Grimaldi, S. (2007) High-stability semiquinone intermediate in nitrate reductase A (NarGHI) from *Escherichia coli* is located in a quinol oxidation site close to heme b_D. *Biochemistry 46*, 5323−5329.

(19) Arias-Cartin, R., Lyubenova, S., Ceccaldi, P., Prisner, T., Magalon, A., Guigliarelli, B., and Grimaldi, S. (2010) HYSCORE evidence that endogenous mena- and ubisemiquinone bind at the same Q site ($Q_{(D)}$) of *Escherichia coli* nitrate reductase A. *J. Am. Chem. Soc. 132*, 5942−5943.

(20) Grimaldi, S., Arias-Cartin, R., Lanciano, P., Lyubenova, S., Endeward, B., Prisner, T. F., Magalon, A., and Guigliarelli, B. (2010) Direct evidence for nitrogen ligation to the high stability semiquinone intermediate in *Escherichia coli* nitrate reductase A. *J. Biol. Chem. 285*, 179−187.
(21) Zhao, Z., Rothery, R. A., and Weiner, J. H. (2003) Transient kinetic studies of heme reduction in *Escherichia coli* nitrate reductase A (NarGHI) by menaquinol. *Biochemistry 42*, 5403−5413.
(22) Zhao, Z., Rothery, R. A., and Weiner, J. H. (2003) Effects of site-directed mutations on heme reduction in *Escherichia coli* nitrate reductase A by menaquinol: A stopped-flow study. *Biochemistry 42*, 14225−14233.
(23) Giordani, R., and Buc, J. (2004) Evidence for two different electron transfer pathways in the same enzyme, nitrate reductase A from *Escherichia coli*. *Eur. J. Biochem. 271*, 2400−2407.
(24) Giordani, R., Buc, J., Cornish-Bowden, A., and Cárdenas, M. L. (1997) Kinetics of membrane-bound nitrate reductase A from *Escherichia coli* with analogues of physiological electron donors: Different reaction sites for menadiol and duroquinol. *Eur. J. Biochem. 250*, 567−577.
(25) Pascal, M. C., Burini, J. F., Ratouchniak, J., and Chippaux, M. (1982) Regulation of the nitrate reductase operon: Effect of mutations in *chlA, B, D* and *E* genes. *Mol. Gen. Genet. 188*, 103−106.
(26) Rothery, R. A., and Weiner, J. H. (1996) Interaction of an engineered [3Fe-4S] cluster with a menaquinol binding site of *Escherichia coli* DMSO reductase. *Biochemistry 35*, 3247−3257.
(27) Bloch, D. A., Borisov, V. B., Mogi, T., and Verkhovsky, M. I. (2009) Heme/heme redox interaction and resolution of individual optical absorption spectra of the hemes in cytochrome *bd* from *Escherichia coli*. *Biochim. Biophys. Acta 1787*, 1246−1253.
(28) Cammack, R. (1996) Redox states and potentials. In *Bioenergetics: A Practical Approach*, pp 85−105, Oxford University Press, New York.
(29) Lanciano, P., Vergnes, A., Grimaldi, S., Guigliarelli, B., and Magalon, A. (2007) Biogenesis of a respiratory complex is orchestrated by a single accessory protein. *J. Biol. Chem. 282*, 17468−17474.
(30) Fedor, J. G., Rothery, R. A., Giraldi, K. S., and Weiner, J. H. (2014) Q-Site occupancy defines heme heterogeneity in *Escherichia coli* nitrate reductase A (NarGHI). *Biochemistry 53*, 1733−1741.
(31) Arias-Cartin, R., Grimaldi, S., Pommier, J., Lanciano, P., Schaefer, C., Arnoux, P., Giordano, G., Guigliarelli, B., and Magalon, A. (2011) Cardiolipin-based respiratory complex activation in bacteria. *Proc. Natl. Acad. Sci. U.S.A. 108*, 7781−7786.
(32) Lanciano, P., Savoyant, A., Grimaldi, S., Magalon, A., Guigliarelli, B., and Bertrand, P. (2007) New method for the spin quantitation of $[4Fe-4S]^{+}$ clusters with $S = {}^{3}/_{2}$. Application to the FS0 center of the NarGHI nitrate reductase from *Escherichia coli*. *J. Phys. Chem. B 111*, 13632−13637.
(33) Rothery, R. A., and Ingledew, W. J. (1989) The cytochromes of anaerobically grown *Escherichia coli*. An electron-paramagnetic-resonance study of the cytochrome *bd* complex *in situ*. *Biochem. J. 261*, 437−443.
(34) Gray, H. B., Stiefel, E. I., Valentine, J. S., and Bertini, I. (2006) *Biological Inorganic Chemistry: Structure and Reactivity*, 1st ed., University Science Book, Sausalito, CA.
(35) Ullmann, G. M., and Knapp, E. W. (1999) Electrostatic models for computing protonation and redox equilibria in proteins. *Eur. Biophys. J. 28*, 533−551.
(36) Fonseca, B. M., Paquete, C. M., Salgueiro, C. A., and Louro, R. O. (2012) The role of intramolecular interactions in the functional control of multiheme cytochromes *c*. *FEBS Lett. 586*, 504−509.
(37) Louro, R. O., Catarino, T., Paquete, C. M., and Turner, D. L. (2004) Distance dependence of interactions between charged centres in proteins with common structural features. *FEBS Lett. 576*, 77−80.
(38) Johansson, M. P., Blomberg, M. R. A., Sundholm, D., and Wikström, M. (2002) Change in electron and spin density upon electron transfer to haem. *Biochim. Biophys. Acta 1553*, 183−187.
(39) Kamiya, K., Yamamoto, S., Shiraishi, K., and Oshiyama, A. (2009) Significant change in electronic structures of heme upon reduction by strong coulomb repulsion between Fe *d* electrons. *J. Phys. Chem. B 113*, 6866−6872.
(40) Tran, Q. H., and Unden, G. (1998) Changes in the proton potential and the cellular energetics of *Escherichia coli* during growth by aerobic and anaerobic respiration or by fermentation. *Eur. J. Biochem. 251*, 538−543.
(41) Quinlan, C. L., Gerencser, A. A., Treberg, J. R., and Brand, M. D. (2011) The mechanism of superoxide production by the Antimycin-inhibited mitochondrial Q-cycle. *J. Biol. Chem. 286*, 31361−31372.
(42) Nicholls, D. G., and Ferguson, S. J. (2003) *Bioenergetics*, 3rd ed., Academic Press, London.
(43) DeLano, W. L. (2002) *The PyMOL Molecular Graphics System*, Schrödinger, LLC, Portland, OR.